PHYSICAL REVIEW B VOLUME 4, NUMBER 4 15 AUGUST 1971

Effect of Magnetic Field on the Energy of Surface Bound States

Joel A. Appelbaum and G. A. Baraff
Bell Telephone Laboratories, Murray Hill, New Jersey 07974
(Received 17 February 1971)

We have performed a self-consistent calculation of the energy levels of electrons bound in the accumulation layer at the surface of a semiconductor in order to determine their dependence on magnetic field. The calculation was performed by solving Poisson's and Schrödinger's equations for the bound states and using a dielectric, i.e., linear-response, formalism to treat the mobile charge. Three different approaches to the dielectric response have been compared. The first treats the dielectric function in a bulk Thomas-Fermi approximation. The second introduces a local, but position-dependent, dielectric function to incorporate the vanishing of the mobile electron wave function at the surface. The third approach uses a nonlocal independent-particle response function for the mobile charge, again including the effect of the surface. We find that the modification of the dielectric function by the surface has a profound effect on the field dependence of the binding energies.

I. INTRODUCTION

During the last few years, there have been a number of theoretical and experimental investigations of the potential which exists near the surface of a semiconductor subject to an external electric field applied perpendicular to its surface. When this potential is sufficiently attractive, it will support bound states—states in which the motion of the electron perpendicular to the surface is limited to a region close to the surface.[1] In the early experimental study of these states,[2–5] the field was in such direction and of such magnitude as to produce an inversion layer at the surface. In such cases, the mobile charge in the bulk is physically separated from the bound surface charge by the energy gap of the semiconductor, as shown in Fig. 1(a). More recently, Tsui[6] has studied the bound states in n-type InAs, where the field is in such direction as to produce an accumulation layer. Here, as shown in Fig. 1(b), the bulk mobile charge is present all the way up to the surface of the semiconductor.

The physical situation in the two cases, inversion layer and accumulation layer, is conceptually different. For the inversion layer, one assumes an electric field at the surface of the semiconductor, postulates a uniform fixed background charge, and allows electronic states in the final self-consistent potential to be occupied up to the Fermi energy. The self-consistent potential arises, via Poisson's equation, from the sources described above. There is, in general, an electric field at the inner edge of the inversion layer and this field is screened out by the fixed charge in the depletion region. The mobile carriers can therefore be ignored in studies of the bound charge. For the accumulation layer, on the other hand, the bound and mobile charges occupy the same regions of space and enter Poisson's equation on an equal footing. The requirement of charge neutrality (the condition that the electric field go to zero far from the surface) enters directly into the determination of the surface potential.

There have been a number of theoretical treatments of the inversion-layer problem. In one of the earliest, done by Handler and Eisenhouer[2] for nearly intrinsic germanium with a p-type inversion layer, the authors remark that the degenerate valence band of germanium contributes two types of carriers, heavy holes and light holes. They assume that the potential is influenced only by background charge and the numerous heavy holes, which they treat in a continuum approximation. This gives them a potential which they use in Schrödinger's equation to determine the energy levels of the light holes. The discrete states play no role in determining the potential at the surface.

In situations where the charge associated with the discrete states becomes large, their role in determining the electrostatic potential must be included. Such a calculation was done by Stern and Howard.[7] In that calculation they included both the discrete-state charge density and the fixed background charge associated with the inversion layer. In the case they treated, the bulk p-type charge density played no role in determining the surface potential. This resulted from their assumption that the width of the depletion layer was exactly such that no field reached the region of mobile charge. A calculation for surface bound states in an accumulation layer was done about the same time by Duke.[8] Duke assumed an exponential surface potential and allowed the two parameters of the potential to be determined by the value of the field at the surface and the decay length for the weakest bound state in that potential. The mobile charge here also played no role in determining the potential.

There has been recent experimental interest in

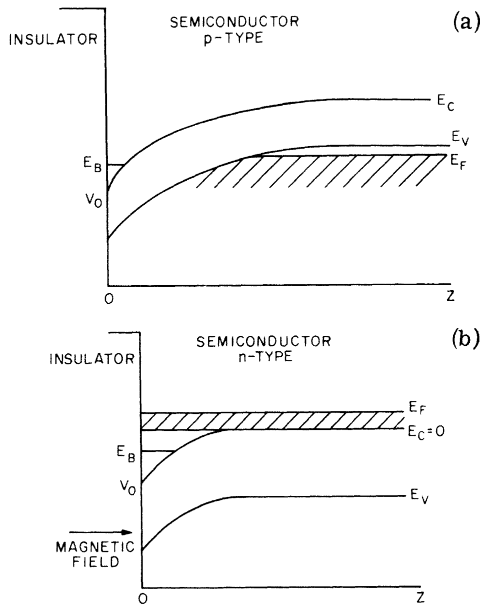

FIG. 1. (a) Schematic representation of the potential in the neighborhood of a p-type semiconductor-insulator interface for an electric field strong enough to support one bound state at energy $-E_B$. (b) Schematic representation of the potential in the neighborhood of a n-type semiconductor-insulator interface for an electric field strong enough to support one bound state at energy $-E_B$. Dashed lines represent filled states of positive energy. The magnetic field indicated is normal to the interface.

the effect of a magnetic field on the energy of these discrete states in accumulation layers.[9] For this reason, we have undertaken a self-consistent calculation of the energy of the discrete states in an accumulation layer in the presence of a magnetic field by solving Poisson's and Schrödinger's equations for the bound states and using a dielectric, i.e., linear-response, formalism to treat the mobile charge. Because of our use of the linear-response formalism, the calculation falls one step short of being fully self-consistent. It does, however, represent the first attempt to include the influence of the mobile electrons on the self-consistent potential in the presence of bound states.

II. MODEL

For the purposes of this investigation, we shall ignore such details as the distribution of fixed charges (if present) in the insulator or at the interface, the polarizability of the insulator, etc. Instead. we shall start the calculation with the assumption that there is a given electric field at $z=0$, the semiconductor-insulator interface, and ask what potential this gives rise to at positive z, in the bulk of the semiconductor.

For definiteness, we shall consider an n-type semiconductor, so that the charges which ultimately shield out the electric field are the conduction electrons and the fixed uniform positive background of ionized donors. The conduction electrons will be treated within the simplest one-band effective-mass formalism. Thus, the specific details of the semiconductor disappear completely, except that the electrons are assigned an effective mass m, and the relation between the electric field and the charges which give rise to it is characterized by a dielectric constant ϵ. Within this simple formalism, one would characterize the interface at $z=0$ as a potential step which would cause the wave functions of the conduction electrons to decay exponentially into the insulator, for $z<0$. There is reason to believe that this potential step is about 0.5–1 eV and therefore that the electronic wave functions are not negligible in the insulator, although they are small there. Nonetheless, it is unlikely that this tailing of the electronic wave function plays an essential role in the phenomena we are considering. We shall, for this reason, treat the potential step as if it were infinite, that is, we shall impose the boundary condition that the conduction-electron wave functions vanish at $z=0$. Thus, the specific characteristics of the insulator are also discarded in this approach. Finally, the last assumption needed to define our model is that the electrons interact with each other only via the self-consistent field—the Hartree approximation. (In the materials of interest for the study of these magnetic effects—small-band-gap semiconductors—the small effective mass and large dielectric constant lead to a small r_s which emphasizes the Hartree term in the interaction relative to exchange and correlation terms.)

In Fig. 1(b) we have sketched the potential energy which an electron experiences in an accumulation layer. It is convenient to let the potential be zero at large z, so that the potential energy at $z=0$ is negative. The Schrödinger equation for this situation is separable. The energy associated with the electron's motion in the z direction may be negative, in which case we speak of it as a bound electron or it may be positive, in which case we speak of it as a mobile electron.

The presence of a magnetic field in the z direction quantizes the motion in the x and y directions so that only discrete values of the transverse energy are to be used. These discrete energies add to the already discrete energies of the bound states so that the total energy of an electron in a bound state, while it may be positive, is still discrete. The electrons in the mobile states have a continuous spectrum of energies made up of the continuous energy for their z motion and the discrete energy imposed on them by the magnetic field. Their response to applied electric fields will exhibit all of the oscillatory phenomena usually

associated with the Landau levels of a system of conduction electrons.

The wave functions and energies for the bound states will be calculated using Schrödinger's, Hartree's, and Poisson's equations. However, the wave function for the mobile states will not be used. Instead, the charge density which they contribute will be calculated using a linear-response formalism to be described in Sec. III.

The equations of our model are the following.

A. Schrödinger's Equation for Bound States

$$[(\vec{p}+e\vec{A}/c)^2/2m+V(z)]\psi(\vec{r})=E\psi(\vec{r}) \quad , \tag{2.1a}$$

$$\psi(z=0)=0 \ , \tag{2.1b}$$

$$\psi(z=\infty)=0 \ . \tag{2.1c}$$

$\vec{A}$ is the vector potential for a uniform magnetic field in the z direction, namely, $\vec{A}=(0, Hx, 0)$. The states ψ have the form

$$\psi_{n,m,k}(r)=(L_y)^{-1/2}e^{iky}\varphi_n(x-x_0)\chi_m(z) \quad , \tag{2.2}$$

where L_y is a normalization length in the y direction, $\varphi_n(x)$ is the nth normalized harmonic-oscillator wave function

$$\left(-\frac{\hbar^2}{2m}\frac{d^2}{dx^2}+\frac{m\omega_c^2x^2}{2}\right)\varphi_n(x)=(n+\tfrac{1}{2})\hbar\omega_c\varphi_n(x) \ , \tag{2.3a}$$

$$\int dx\ \varphi_n(x)\varphi_m(x)=\delta_{nm} \quad , \tag{2.3b}$$

and

$$\omega_c\equiv eH/mc \quad , \tag{2.3c}$$

$$x_0\equiv-\hbar k/m\omega_c \ . \tag{2.3d}$$

The total energy of the state,

$$E_{n,m,k}=(n+\tfrac{1}{2})\hbar\omega_c+\epsilon_m \quad , \tag{2.4}$$

and the bound-state wave function $\chi_m(z)$ are determined by the one-dimensional Schrödinger equation

$$\left(-\frac{\hbar^2}{2m}\frac{d^2}{dz^2}+V(z)\right)\chi_m(z)=\epsilon_m\chi_m(z) \quad , \tag{2.5a}$$

$$\chi_m(0)=0 \quad , \tag{2.5b}$$

$$\chi_m(\infty)=0 \ . \tag{2.5c}$$

B. Poisson's Equation for Potential

The potential energy $V(z)$ appearing in (2.1) is taken to be the energy of an electron in a potential $U(z)$, $V(z)=-eU(z)$, where U is the electrostatic potential which satisfies Poisson's equation

$$-\frac{d^2}{dz^2}U(z)=\frac{4\pi}{\epsilon}[\rho_b(z)+\rho_m(z)] \ , \tag{2.6a}$$

$$U(\infty)=0 \ , \tag{2.6b}$$

$$\left(\frac{-dU}{dz}\right)_0=-\frac{4\pi\sigma_s}{\epsilon} \ . \tag{2.6c}$$

Here ϵ is the background dielectric constant of the semiconductor, ρ_b is the charge associated with the bound states described in (2.1)–(2.5), ρ_m is the charge associated with the mobile charge, and σ_s is the surface charge which we use to represent the fixed value of electric field at $z=0$.

C. Equation for Charge Density

The charge density associated with the bound states may be written, for a noninteracting system, as

$$\rho_b(z)=-2e\int d\omega\sum_n\sum_m\sum_k\psi^*_{nmk}(r)\psi_{nmk}(r)\times\delta(E_{nmk}-\omega)f_T(\omega-\mu). \tag{2.7}$$

Here, the factor of 2 arises because of spin. The function $f_T(\omega-\mu)$ is the probability that a state of energy ω is occupied when the Fermi energy is μ, the temperature is T, and the δ function is the spectral density of states. We shall always be working at zero temperature, where f_T is the unit step function, taking the value zero if $\omega>\mu$ and unity otherwise. Allowing the electronic states to have finite lifetimes, such as would be produced by scattering, is represented by softening the δ function δ into a function δ_B (to be defined in Sec. III) of finite width and height.

Returning to (2.7), we replace the sum over k by an integral. Using periodic boundary conditions over the normalization length L_y,

$$\sum_k\rightarrow L_y/2\pi\int dk \ ,$$

replacing the k integration by an integration over x_0, using the normalization (2.3b) of the harmonic-oscillator wave functions, and using the expression (2.4) for the energy, we obtain

$$\rho_b(z)=-\frac{e}{\pi}\frac{m\omega_c}{\hbar}\int_{-\infty}^{\mu}d\omega\sum_n\sum_m\chi_m^2(z)\times\delta_B[\epsilon_m+(n+\tfrac{1}{2})\hbar\omega_c-\omega]$$

$$=-\frac{e}{\pi}\frac{m\omega_c}{\hbar}\sum\chi_m^2(z)N(\mu-\epsilon_m) \ , \tag{2.8a}$$

where

$$N(\mu-\epsilon_m)\equiv\sum_n\int_{-\infty}^{\mu}\delta_B[\epsilon_m+(n+\tfrac{1}{2})\hbar\omega_c-\omega]d\omega \ . \tag{2.8b}$$

The mobile charge density is, strictly speaking, given by an expression like (2.7) in which mobile states replace the bound states ψ minus the background charge density. Instead of evaluating this exactly we proceed as though the resultant density can be represented as a linear response to the potential,

$$\rho_m(z) = \int_0^\infty \tilde{R}(z, z')V(z')dz' \quad , \tag{2.9}$$

where $\tilde{R}(z, z')$ is a response kernel which is independent of V. Such an approach is equivalent to the use of first-order perturbation theory. Although it is justified when the potential is small enough, its use in this problem, where the potential is large enough to support bound states, is undoubtedly the weakest point in our approach. Clearly, the response kernel $\tilde{R}$ will depend on the magnetic field H. This dependence provides an important coupling between the magnetic field and the potential in the accumulation layer.

Before proceeding to the description of the approximation used for the response kernel, let us introduce the dimensionless units which will be used in the calculation.

All energies will be expressed in multiples of $\hbar^2/2m$, which means that energy takes the dimension L^{-2}. The scale of the problem is such that it is convenient to use 100 Å as the unit of length. We shall use E_F to denote the Fermi energy μ, E_H to denote the magnetic energy $\hbar\omega_c$, and E_m to denote the z energy ϵ_m in these units. The potential energy will be denoted by $\phi(z)$. We express charge densities such as ρ_b and ρ_m as number density (units L^{-3}), which introduces a unit of inverse length

$$K_0 \equiv 8\pi m e^2/\epsilon\hbar^2 \tag{2.10}$$

into Poisson's equation. The equations we will solve are, in the new notation,

$$-\frac{d^2}{dz^2}\,\phi(z) = K_0 \left\{ \frac{E_H}{2\pi} \sum_m \chi_m^2(z) N(E_F - E_m) + \int_0^\infty R(z, z')\,\phi(z')dz' \right\} , \tag{2.11a}$$

$$\phi(\infty) = 0 \quad , \tag{2.11b}$$

$$\frac{d\phi}{dz}\; z = 0 = K_0 N_s \quad , \tag{2.11c}$$

where N_s is a fixed surface charge density, and

$$\left(-\frac{d^2}{dz^2} + \phi(z)\right)\chi_m(z) = E_m\,\chi_m(z) \quad . \tag{2.12}$$

III. LINEAR-RESPONSE FORMALISM

In this section we will consider three separate approximations in treating the mobile electron response. The three approximations represent successively more sophisticated approaches to electron screening at the surface of a metal or degenerate semiconductor. As we shall see, they behave qualitatively differently in a magnetic field. All three fall within the linear-response formalism, ignoring exchange and correlation. Since, as we discussed previously, r_s is small (typically, $r_s < 0.5$), this approximation of ignoring exchange and correlation is a good one. The first case we consider is the usual bulk Thomas-Fermi approximation. This has been studied by a number of authors.[10] We include it here for completeness and also to present the results in the presence of lifetime broadening. The second and third approximations, which we call surface Thomas-Fermi (STF) and nonlocal, explicitly include the influence of the surface on the electron screening. This problem has been discussed recently by Newns[11] in the absence of a magnetic field, and without lifetime broadening.

A. Bulk Thomas-Fermi Approximation

In general, i.e., within linear-response theory, the induced charge density $\delta\rho(\vec{x})$ is related to the applied potential $\delta V(\vec{x}')$ by

$$\delta\rho(\vec{x})\,\alpha \int R(\vec{x}, \vec{x}')\delta V(x')d^3x' \quad . \tag{3.1}$$

If $\delta V(x')$ is slowly varying it can be taken outside the integral sign and one obtains the local approximation

$$\delta\rho(\vec{x}) = \delta V(\vec{x}) \int R(\vec{x}, \vec{x}')d^3x' \quad , \tag{3.2}$$

$$\delta\rho(z) \equiv \delta V(z) K^2(z) \quad . \tag{3.3}$$

If, in addition, the system is uniform, $\vec{K}^2(\vec{x})$ is independent of $\vec{x}$ and it can be determined by considering the limit in which $\delta V(\vec{x})$ is constant. The induced charge density in this case is just the same as that which would result from shift in the Fermi energy E_F by δV, i.e., $N(E_F)\delta V$, where $N(E_F)$ is the density of state at the Fermi level. From this we get the familiar result that

$$K^2 = N(E_F) \quad . \tag{3.4}$$

This relation is equally valid in the presence or absence of a magnetic field.

The energy levels of an electron in a magnetic field are

$$E_{n,k_z} = E_H(n + \tfrac{1}{2}) + k_z^2 \quad , \tag{3.5}$$

and consequently the density of states

$$N(\epsilon) = \frac{E_H}{2\pi} \sum_{n,k_z} \delta(\epsilon - E_{n,k_z}) \quad . \tag{3.6}$$

Doing the k_z integration, one obtains

$$N(E_F) = \frac{E_H}{2\pi^2} \sum_{n=0} \frac{1}{k_n} \quad , \tag{3.7}$$

$$k_n = [E_F - E_H(n + \tfrac{1}{2})]^{1/2} \quad , \tag{3.8}$$

and the sum on n going over all n for which k_n is real. As shown in Fig. 2, this leads to a density of states which exhibits square-root singularities as a function of magnetic field.

These singularities are clearly not present ex-

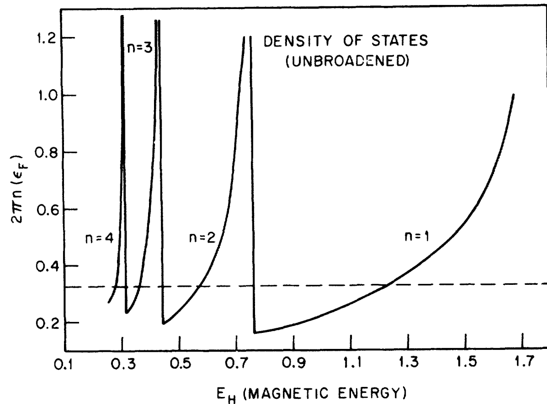

FIG. 2. Density of states at the Fermi energy vs magnetic field for a free-electron gas without lifetime broadening. The square-root singularities as the Landau level passes through the Fermi energy have been cut off for clarity. Horizontal line indicates zero-field density of states. (The energy plotted here is equal to $2\times10^{-12}m/\hbar^2$ times the actual energy in ergs because we have expressed energies as multiples of $\hbar^2/2m$ and have chosen 100 Å as the unit of length. The density of states is that appropriate to these units.)

perimentally, the infinite shielding they imply would result in zero-field penetration and therefore loss of the bound states. Including them would distort the magnetic field dependence of the bound-states energies. We have therefore removed them by introducing lifetime broadening into the calculation of $N(\epsilon)$. This was effected by smearing the δ function in (3.6). The usual procedure has been to use the prescription

$$\delta(\epsilon - x) \to \frac{d/\pi}{(\epsilon - x)^2 + d^2} \quad . \tag{3.9}$$

This proved unsatisfactory, for while it leads to a well-behaved result for $N(E_F)$, the density of states acquires a low-energy tail which makes it impossible to calculate the Fermi energy E_F as a function of E_H from the broadened $N(\epsilon)$. To remove this deficiency, we use instead of (3.9) the prescription

$$\delta(\epsilon - x) \to \frac{2d^3/\pi}{(\epsilon - x)^4 + d^4} \quad . \tag{3.10}$$

The k_z integration in (3.6) can then be done by contours, and one finds

$$N(E) = \frac{N^0(E)}{\sqrt{E}} \; E_H \sum_{n=0} \mathrm{Im}\left(\frac{1+i}{4}\right) \times \left(\frac{1}{k_+(E-E_n)} + \frac{1}{k_-(E-E_n)}\right) \quad , \tag{3.11}$$

where $N^0(\epsilon)$ is the three-dimensional density of states at zero field, $E_n = E_H(n+\frac{1}{2})$, and $k_\pm(x)$ are the complex functions

$$k_+(x) = [x + 2^{-1/2}(1+i)d]^{1/2}, \quad \mathrm{Im}k_+ > 0 \tag{3.12a}$$

and

$$k_-(x) = [x - 2^{-1/2}(1+i)d]^{1/2}, \quad \mathrm{Im}k_- < 0 \quad . \tag{3.12b}$$

In Fig. 3 we have plotted $2\pi K_0 K^2$, which is proportional to $N(E_F)$ vs magnetic field for a broadening $d = 0.1$. Notice how the quantum oscillations in K^2 increase their amplitude as the magnetic field is increased, until finally K^2 becomes a monotonically increasing function of E_H in the extreme quantum limit (i.e., when there is only a single Landau level occupied). The latter behavior results from the steady approach of the last Landau level to the Fermi energy.

In the absence of broadening it is easily seen how K^2 depends on E_H in the extreme quantum limit (EQL). The density of electrons in the system is

$$N = \frac{E_H}{2\pi^2} \sum_{n=0} \dot{k}_n \quad . \tag{3.13}$$

In the EQL this leads to

$$k_0 = \frac{2\pi^2 N}{E_H} \quad .$$

Since

$$K^2 = \frac{E_H^2}{8\pi^4 N} \tag{3.14}$$

we see that K^2 increases as a quadratic function of E_H.

B. Surface Thomas-Fermi Approximation

Near the surface of the semiconductor the mobile electron density is not uniform. The quantity $K^2(z)$ depends on z, the distance from the surface. If we use the same reasoning as we used in Sec. II we arrive at the result

$$K^2 = N(z, E_F) \quad , \tag{3.15}$$

where $N(z, E_F)$ is just the position-dependent density of states at the Fermi energy, defined as

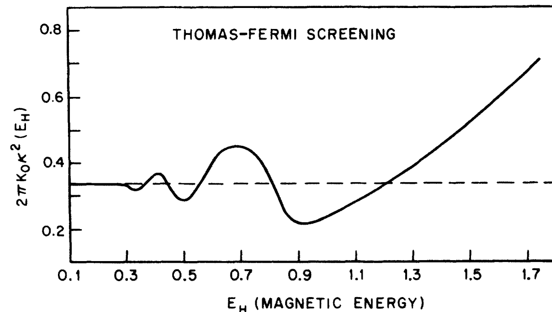

FIG. 3. Square of the Thomas-Fermi screening constant multiplied by 2π (the unit of length is 100 Å) plotted vs magnetic energy. For the material constants considered in the text: 1 unit = 18.8 meV = 32.5 kOe.

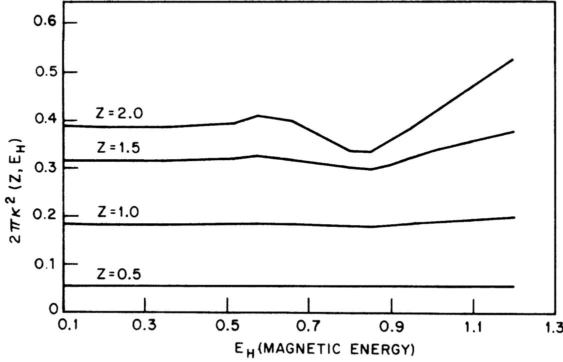

FIG. 4. STF screening function times $2\pi/K_0$ plotted vs magnetic energy E_H for several distances from the surface of the semiconductor. (The energy plotted here is equal to $2\times10^{-12}m/\hbar^2$ times the actual energy in ergs because we have expressed energies as multiples of $\hbar^2/2m$ and have chosen 100 Å as the unit of length.)

$$N(\vec{x}, E_F) \equiv \frac{\partial N(\vec{x})}{\partial E_F} \qquad (3.16)$$

$$= \sum_i |\psi_i(\vec{x})|^2 \delta(E_F - E_i) \ , \qquad (3.17)$$

where $\psi_i(\vec{x})$ is the wave function for an electron with energy E_i.

For the model we have adopted for the surface in Sec. II, $\psi_i(\vec{x})$ takes the form

$$\psi_i(\vec{x}) = (2/L)^{1/2} \sin k_z z \, \phi_n(x - x_0) e^{iky} \ , \qquad (3.18)$$

where $\phi_n(x)$ is the harmonic-oscillator wave function. After integrating over k, we obtain

$$K^2(z) = \frac{E_H}{\pi L} \sum_{nk_z} \sin^2 k_z z \, \delta(E_F - E_n - k_z^2)$$

$$= \frac{1}{2\pi^2} E_H \sum_n \frac{\sin^2 k_n z}{k_n} \ . \qquad (3.19)$$

There are a number of interesting things to notice about (3.19). In the small z, limit $K^2(z)$ takes the form

$$K^2(z) \approx (1/2\pi^2)(E_H \textstyle\sum_n k_n) z^2 \ . \qquad (3.20)$$

This is independent of magnetic field, since, from (3.13), the term in parentheses is simply proportional to the number of electrons in the Fermi sea. The screening charge at the surface of a metal, within the local approximation, is consequently independent of magnetic field! What is happening here is that the total charge density is oscillating towards and away from the surface of the metal in just such a way as to cancel the oscillation in the electron density of states.

Once again we felt it necessary to introduce lifetime broadening into the problem. This was done in precisely the same manner as in Sec. III A by smearing the δ function. In this way, one obtains

$$K^2(z) = \frac{E_H}{2\pi^2} \sum_n \mathrm{Im}(1+i) \times \left(\frac{1 - e^{2ik_+ z}}{k_+} + \frac{1 - e^{-2ik_- z}}{k_-} \right) \ , \qquad (3.21)$$

where

$$k_\pm \equiv k_\pm(E_F - E_n) \ .$$

This is plotted in Fig. 4 as a function of magnetic field for various values of z. Notice that K^2 does not become field dependent until one has gone two units (200 Å) into the semiconductor.

C. Nonlocal Screening

If the potential $V(\vec{x})$ varies on the scale of the response kernel $R(\vec{x}, \vec{x}')$, removing it from the integral in (3.1) is no longer permissible. It is now necessary to have detailed knowledge of $R(\vec{x}, \vec{x}')$. Using the random phase approximation (RPA)[11] and (3.18) for the electron wave functions, one obtains

$$R(z, z') = E_H \sum_n \sum_{\substack{k_z > 0 \\ k_z' > 0}} \frac{f(E_{n,k_z}) - f(E_{nk_z'})}{E_{n,k_z} - E_{n,k_z'}} \times \sin k_z z \sin k_z' z \sin k_z z' \sin k_z' z' \ , \qquad (3.22)$$

where $f(E)$ is the Fermi-Dirac distribution function.

A self-consistent solution to the screening problem would involve introducing (3.1) into Poisson's equation and then performing a numerical solution to the integrodifferential equation which would result. Considering the complexity of the kernel in (3.22), a direct attack on this problem seems particularly unpromising unless considerable analytic simplification of the expression for the induced charge can be effected. To this end we found[12] that an exponential parametrization of the potential $V(x)$ allows a rather simple expression to be obtained for the induced charge. This can then be used for an iterative solution to Poisson's equation.

In Ref. 12 we show that the charge resulting from a potential

$$V(z) = -V_0 e^{-\lambda z} \qquad (3.23)$$

is

$$\rho(z) = -\frac{V_0}{2\pi^2} E_H \sum_{n=0}^{N_{\max}} \left(\frac{1 - e^{-\lambda z}}{\lambda} \int_0^{2k_n} \frac{t \sin zt}{t^2 + \lambda^2} \, dt - e^{-\lambda z} \int_0^{2k_n} \frac{1 - \cos zt}{t^2 + \lambda^2} \, dt \right) \ . \qquad (3.24)$$

Notice that $\rho(z)$ at large distances consists of two parts, one of which decays exponentially in the same way as the potential, the other of which exhibits long-range Friedel oscillations. The Frie-

del oscillations decay at large z as

$$\rho(z) \approx -\frac{V_0}{2\pi^2} E_H \sum_{n=0}^{N_{\max}} \frac{\cos 2k_n z}{z} \frac{2k_n}{(2k_n)^2+\lambda^2} , \quad (3.25)$$

the $1/z$ decay being typical of one-dimensional systems. For small z, $\rho(z)$ can be expanded in powers of z and one finds

$$\rho(z) = -\frac{V_0}{2\pi^2} E_H \sum_n k_n \left(1 - \frac{\lambda}{2k_n} \tan^{-1} \frac{2k_n}{\lambda}\right) z^2 . \quad (3.26)$$

This behaves quite differently depending on the relative sizes of k_n and λ. For λ small compared to k_n the leading term is just $E_H \sum k_n$, which is exactly the result we obtained in the surface Thomas-Fermi (STF) approximation. This of course is not surprising, for it is just this regime in which the local approximation is valid.

In the nonlocal regime, where $\lambda > k_n$,

$$\rho(z) = -\frac{V_0}{2\pi^2} \left(E_H \sum_n \frac{4k_n^3}{3\lambda^2} \right) z^2 . \quad (3.27)$$

In the EQL, the z^2 coefficient is a rapidly decreasing function of magnetic field, decreasing as $1/E_H^2$. This behavior comes about from the movement of the electron charge away from the surface in the EQL. The same movement occurred in the STF approximation but here, in the fully nonlocal treatment, the electron density enters into the expression for the induced charge twice, once because we are asking for the induced charge in a region where the density is small, and again because the actual perturbation strength is proportional to the product of the charge density and the potential. In the local approximation one assumes the potential is sufficiently long range that it couples to the average or bulk density, and not the surface density, and hence the density only enters once.

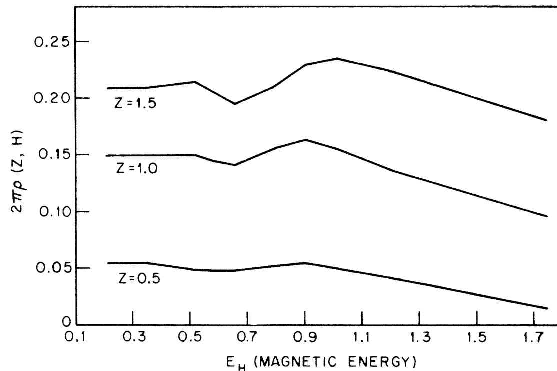

FIG. 5. Induced mobile charge caused by a potential of the form $V=e^{-\alpha z}$ with $\alpha=1.1$ plotted as a function of magnetic energy E_H for several values of z. (The energy plotted here is equal to $2\times10^{-12} m/\hbar^2$ times the actual energy in ergs because we have expressed energies as multiples of $\hbar^2/2m$ and have chosen 100 Å as the unit of length. The density of states is that appropriate to these units.)

In Fig. 5 we have plotted $\rho(z)$ vs E_H for various z. Notice the decrease in screening charge as the magnetic field increases in the EQL. This should be contrasted with the increase in screening in the bulk Thomas-Fermi approximation and the field independences of the STF approximation in this same limit.

IV. CALCULATION

The calculation we shall describe is basically a numerical one. As it turned out, there were significant differences in procedure required by the Thomas-Fermi and STF approximations on the one hand and the nonlocal screening approximation on the other. Let us first describe certain important features common to both sets of calculations.

A. Iteration Scheme

The basic method of handling Eqs. (2.11) and (2.12) was iterative: We assumed a starting potential, calculated bound-state energies and wave functions and used these to calculate the bound charge density. The mobile charge density was evaluated and we were left with Poisson's equation (or a modified Poisson's equation as we shall explain later), from which a new potential was obtained by numerical integration inward from large z. Self-consistency is achieved when the new potential is sufficiently close to the old. As a practical matter, we used the new potential to compute new bound-state energies and stopped iterating when each of the new energies differed from its old counterpart by less than 1%.

The principal decision in such a scheme is the choice of the potential to be used in starting the next round of iterations, as Stern has so clearly discussed.[13] We chose, as input to the $(n+1)$th round of iterations, a potential equal to a fraction $(1-f)$ of the input potential to the nth round plus a fraction f of the output potential from that nth round. Since too small an f gives slow convergence and too large an f gives oscillations (and often divergence), we presume that keeping f at the largest value which provides monotonic convergence will give the fastest convergence. To this end, we had the computer store the three most recently computed values of the lowest bound-state energy. If these showed monotonic progress, f was increased by a factor of 1.125. If these showed oscillatory progress, f was decreased by a factor of 0.8. In all cases, f was not allowed to become smaller than 0.1 nor larger than 1.0. The method led to values of f near 0.4 on the final iteration.

B. Eigenvalues and Eigenfunctions

For the purpose of streamlining the calculation, eigenvalues were calculated using the WKB method and these eigenvalues, used in the Schrödinger wave equation, allowed us to calculate the corresponding wave function by an inward integration. The measure of accuracy of the eigenvalues is provided by the smallness at the origin of the wave function calculated in this way, the exact eigenvalue (no matter how it is obtained) leading to a wave function which vanishes at the origin. We estimate that errors due to this approximation are less than 1%.[14]

C. Lifetime Broadening of Bound States

In Sec. III A, we discussed in connection with the linear response of the mobile charge, the replacement of the δ function in the spectral density by a broadened δ function. It was necessary for us to use this same procedure when we calculated the bound charge density. Had we not done so, we would have found that the total amount of bound charge changes discontinuously as the energy of one of the bound Landau levels $E=E_m+(n+\frac{1}{2})E_H$ passes through the Fermi level. We used the same broadened δ function, with the same broadening parameter, for both the bound charge and the mobile charge.

There is a significant difference in our numerical treatment of the two local-screening approximations and the single nonlocal-screening approximation. In the local-screening approximation, Eq. (2.11) can be rewritten as

$$-\left(\frac{d^2}{dz^2}-K^2(z)\right)\phi(z)=\frac{K_0E_H}{2\pi}\sum_m \chi_m^2(z)N(E_F-E_m) \ , \tag{4.1a}$$

where

$$K^2(z)=-\frac{K_0E_H}{2\pi}\int_0^\infty R(z,z')dz' \ , \tag{4.1b}$$

$$\phi(\infty)=0 \ , \tag{4.1c}$$

$$\left(\frac{d\phi}{dz}\right)_0=K_0N_s \ . \tag{4.1d}$$

The potential is to be calculated by solving (4.1). We do this by choosing some large value of z at which $\chi_m^2(z)$ is negligible, setting $\phi(z)=0$ and $\phi'(z)=0$ at this point and integrating (4.1a) inward. The potential so obtained satisfies (4.1c) but, in general, does not satisfy (4.1d). However, we have obtained in this way a particular integral of (4.1a) and we can always add to this any multiple of the solution to the homogeneous equation. We add just as much of the homogeneous solution as is needed to satisfy boundary condition (4.1d). To obtain the homogeneous solution of (4.1a), we choose values of z large enough that $K^2(z)$ is constant, so that beyond that value of z, the two homogeneous solutions behave as $e^{\pm zK}$. We use the solution which goes as e^{-zK} at large z and integrate the homogeneous equation numerically towards smaller z.

In the case of nonlocal screening, the calculation is completely different. The first step in the computation of the mobile charge is to replace the actual potential $\phi(z)$ by its parametrized form

$$\phi(z)\to -V_0e^{-\lambda z} \ . \tag{4.2}$$

Let us stress that this replacement is *not* used in the calculation of the bound-state energies. The two parameters of the potential, V_0 and λ, have to be adjusted so that the parametrized form is a reasonable approximation to the true potential it replaces. There are various ways in which this can be accomplished. However, there is one constraint which *must* be imposed on V_0 and λ, a constraint which bears no obvious relation to the shape of the potential but which must be satisfied if we are to obtain a solution to (2.11), namely, the total amount of induced charge must be such that the sum of the integrated mobile charge and the integrated bound charge is just the charge needed to give zero electric field in the bulk of the semiconductor.

To see in more detail what this condition leads to, consider (2.11a). On the right-hand side, we replace $\phi(z)$ by its parametrized form (4.2), obtaining

$$-\frac{d^2}{dZ^2}\phi(z)=\frac{K_0E_H}{2\pi}\left(\sum_m \chi_m^2(z)N(E_F-E_m)-V_0F(z,\lambda)\right), \tag{4.3}$$

where $F(z,\lambda)$ is the function which appears in (3.24), namely,

$$F(z,\lambda)=\sum_{n=0}^{N_{\max}}\left(\frac{1-e^{-\lambda z}}{\lambda}\int_0^{2k_n}\frac{t\sin zt}{t^2+\lambda^2}\,dt-e^{-\lambda z}\int_0^{2k_n}\frac{1-\cos zt}{t^2+\lambda^2}\,dt\right) . \tag{4.4}$$

Note that

$$\int_0^\infty dz\,F(z,\lambda)=\frac{1}{\lambda}\sum_{n=0}^{N_{\max}}\frac{2k_n}{4k_n^2+\lambda^2}\equiv Q(\lambda) \ . \tag{4.5}$$

We integrate (4.3) from $z=0$ to $z=\infty$, using the boundary conditions (2.11b) and (2.11c) with the result that

$$N_s=E_H\left[\textstyle\sum_m N(E_F-E_m)-V_0Q(\lambda)\right] \ . \tag{4.6}$$

It is this relation between V_0 and λ which must be satisfied. Having done so, we then can integrate (4.3) inward to obtain the potential.

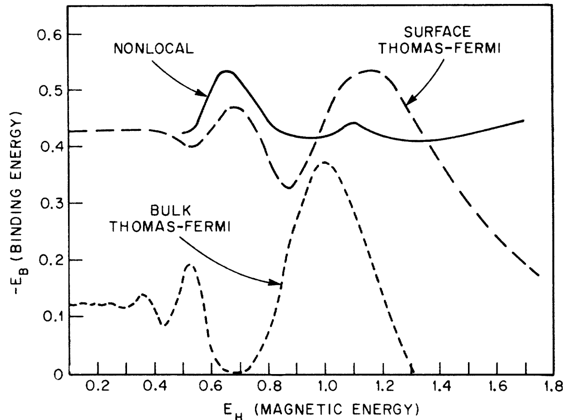

FIG. 6. Binding energy of the single bound state is plotted vs magnetic energy for the three approximations used for the mobile charge response. (The energy plotted here is equal to $2\times10^{-12}m/\hbar^2$ times the actual energy in ergs because we have expressed energies as multiples of $\hbar^2/2m$ and have chosen 100 Å as the unit of length.)

This constraint leaves us free to apply only one fitting condition which we choose to be the requirement that the parametrized potential and actual potential agree at $z=0$.

In order to assess how sensitive our results are to this particular scheme, we used a second parametrization, namely,

$$\phi(z)\rightarrow[V_0/(1-\alpha)](e^{-\lambda z}-\alpha e^{-2\lambda z}) \quad , \qquad (4.7)$$

in which there are three parameters. We must still satisfy the constraint which is equivalent to (4.5) but now we have two free parameters left. These were set by requiring the true potential and the parametrized form to have the same value and slope at $z=0$. While this improved parametrization of the potential resulted in a closer fit to the actual potential, the shapes of the curves of the binding energies E_m vs magnetic field, our primary concern here, were essentially unaffected.

V. RESULTS AND DISCUSSION

Our main concern in this paper is to understand the magnetic field dependence of the bound-state energy E_B. In Fig. 6 we have plotted that energy as a function of magnetic field for the three separate approximations already discussed. The electric field at the surface was chosen so that only one bound state existed in the potential well. This simplifies our task of trying to understand the rather complicated structure exhibited by these curves. The parameters we used for this calculation are $E_F=1.06$, $K_0=7.30$, $N_s=0.33$, and a broadening parameter $d=0.1$.

The magnetic field influences E_B through two separate mechanisms. The first is through the modification of the mobile electron screening, as has been discussed somewhat in Sec. III. The second is through the introduction of magneto-oscillations of the bound charge density caused by change in the number of filled bound-state Landau levels. The shape of the bound charge density, unlike the shape of mobile charge density, is not directly influenced by the magnetic field.

Let us start our analysis with the bulk Thomas-Fermi approximation. The curve exhibits strong magneto-oscillation above $E_H=0.3$. Near $E_H=0.68$ and for $E_H>1.3$ the potential no longer supports a bound state. Some of the structure in the curve is clearly identified as arising from the oscillations in K^2. For example, let us focus on the dip in E_B near $E_H=0.68$. An examination of the screening function K^2 shows that there is a large increase in K^2 (caused by the second Landau level going through the Fermi surface) in precisely this vicinity. This leads to a shorter-ranged potential, and for a fixed electric field at the surface, a shallower potential, which decrease the binding energy. For this particular dip it turns out that the variation of the bound charge density plays no role. To see this in more detail, consider the amount of charge in a bound state. In Fig. 7 we have plotted [using Eq. (2.8b)] the total charge (solid line) in a bound state with energy $-E_B$ versus magnetic field. (The dashed line represents the same information for no broadening.) An examination of Fig. 7 reveals that near $E_H=0.68$, and $E_B=0$, the charge density in the bound state is almost exactly equal to its zero-field value. Change of bound charge therefore plays no role in producing this dip. The strong decrease in binding energy above $E_H=1.0$ is due to a simultaneous increase in K^2 and an increase in

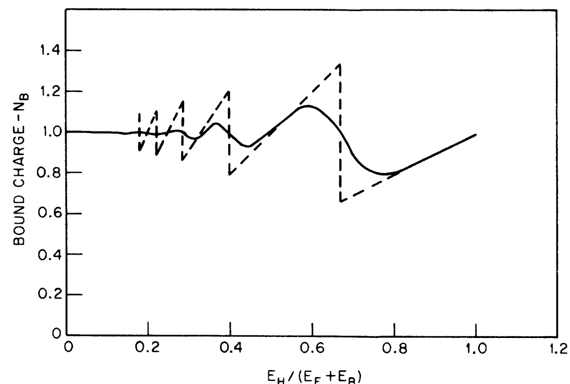

FIG. 7. Plotted here is the total charge contained in a bound state with binding energy $-E_B$, in a system with Fermi energy E_F and magnetic energy E_H. The dashed curve depicts this information in the absence of lifetime broadening. Notice the precipitous drop in bound charge each time a Landau level passes through the Fermi energy. The solid curve was calculated assuming that the lifetime broadening parameter (see text) is 0.1.

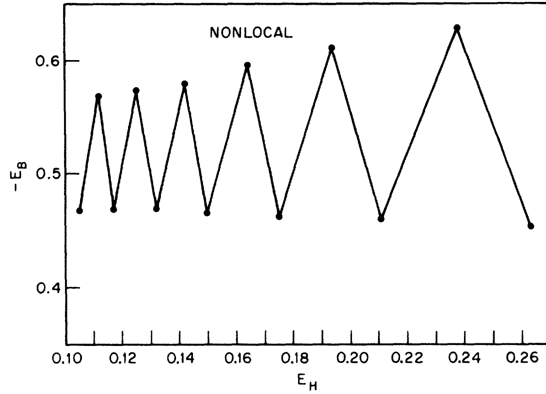

FIG. 8. Bound-state energy $-E_B$ plotted vs magnetic energy E_H for the nonlocal approximation in the low-field regime. Notice the rapid oscillation caused solely by the passage of the unbroadened bulk Landau levels through the Fermi surface. Introducing reasonable lifetime broadening ($\alpha = 0.1$), would completely surpress these oscillations. (The energy plotted here is equal to $2\times10^{-12}m/\hbar^2$ times the actual energy in ergs because we have expressed energies as multiples of $\hbar^2/2m$ and have chosen 100 Å as the unit of length.)

the bound-state charge density as a function of magnetic field. The two prominent peaks in the curve at $E_H = 0.52$ and 1.0 are due to a decrease in K^2 in those neighborhoods as well as decreases in the bound charge. These two effects do not happen to occur at exactly the same field values. This accounts both for the skewed shape of the peak at 0.52 and the shift of both peaks to slightly higher field values than those at which K^2 is most reduced. The remaining structure in the curve at low fields is similarly explained.

We turn now to the STF screening approximation. The first thing to notice is that $-E_B$ lies above that for the bulk approximation. This is easily understood from the fact that the screening in the STF approximation is considerably poorer, in the vicinity of the surface, than in the bulk approximation because of the requirement in STF that the mobile charge density vanish at the surface. This results in a deeper and wider potential. In understanding the magnetic field dependence of the STF curve it is important to notice that mobile electron screening contributes very little structure. As we discussed in Sec. III B, the screening at the surface is only a weak function of magnetic field. Recall that motion of the mobile electron density is such that it just cancels any change in the density of states. This can be seen clearly in Fig. 4 where $K^2(z)$ is plotted versus magnetic field for different values of z. Beyond $z = 2$, the potential is sufficiently weak so that the behavior of K^2 has no significant influence. The peaks and dips in E_B are produced solely by the oscillation in bound charge density. For example, the peak at 1.15 is due to a dip in N_B at $E_H/(E_F - E_B) = 0.76$ (see Fig. 7). Similarly, the dip at $E_H = 0.86$ is due to the peak in N_B at $E_H(E_F - E_B) = 0.59$ and so for the remaining structure.

Finally, consider the nonlocal approximation. Because of the already complex numerical situation, we have neglected broadening in the calculation of the mobile charge response although the bound charge is broadened just as before.

Let us consider first the low-field regime. In Fig. 8 we have plotted the bound-state energy vs magnetic field for low fields. The points represent the value for which E_B was calculated, the lines connecting the points are just for guiding the reader's eye and do not represent the actual continuous curve of E_B vs E_H. The rapid oscillations exhibited by this curve are caused by the motion of the unbroadened mobile charge Landau levels through the Fermi surface. This structure was suppressed by broadening in the previous approximations. Notice that the average value of this curve lies somewhat above that of the STF approximation. This is to be expected since there is effectively less screening charge near the surface in the nonlocal screening approximation than there is in the local screening approximation. For higher field values (See Fig. 6) the curve exhibits two peaks in the same regions where they occur in the STF approximation. As before, this is caused by the bound-state charge oscillations. The major difference between the nonlocal and STF approximations occurs at high field values, where the nonlocal E_B does not decrease with field as it does for the STF and bulk Thomas-Fermi approximations. This is because of the decrease in mobile electron screening which occurs in the extreme quantum regime for the nonlocal approximation. This counteracts the increase in screening due to the bound charge density, leaving the curve of E_B vs E_H a weak function of magnetic field.

Let us discuss now the limitations of the model calculation just presented and the modifications we would expect from an improved treatment. We will focus our attention here on the two surface approximations, STF and nonlocal, since it is clear that the bulk Thomas-Fermi is inadequate for treating screening at the surface.

Probably the most unjustifiable approximation we have made is using a linear-response formalism for calculating the mobile charge. The potential is considerably larger than the Fermi energy and therefore the usual justification for linear-response theory is totally lacking. The potential is in fact so strong that it supports bound states. The bound state already contains a significant fraction of the charge needed to completely screen the electric field. The response of the mobile electrons is

only large enough to supply the remaining fraction. This feature is correctly included in our calculations. What has been left out of our calculation is a *further* exclusion of mobile charge from the surface region which is brought about by the requirement that the mobile electrons be orthogonal to the bound states. The major change we would expect from a nonlinear treatment of screening is an increase in bound-state energies due to this further exclusion of mobile charge.

There are a number of limitations inherent in the model itself. The first of these is our assumption of an infinite potential step at the edge of the semiconductor. This will have two effects. The penetration of electron charge density into the insulating barrier will reduce the depth of the potential well in the semiconductor. On the other hand, the bound states in a given potential will move downwards as the height of the step is reduced. The net motion of the bound-state energies due to these two effects is difficult to assess but we see no mechanism by which this should influence the magnetic field dependence of the bound states.

Tsui's measurements of the field dependence of the binding energy in n-type InAs show a definite increase of the binding energy at low magnetic field and small Fermi energy. In some of the units Tsui studied, this increase was of the order of 50 meV from 0 to 30 kOe.

In an attempt to make a comparison with Tsui's work, we chose input material constants which correspond to those of InAs at a doping level of 2×10^{16} atoms/cm^3. (This corresponds to a Fermi level of 20 meV.) In the experimental units referred to above, the electric field at the surface of the semiconductor was sufficiently strong that two bound states, one at 200 meV and the other at 50 meV, were observed.

We have performed calculations using the STF approximation and electric fields large enough to support bound states at approximately these energies. We found nothing in those calculations that differed substantially from what we have presented here; in particular the binding energies show no increase at low magnetic fields. We do not expect that removing any of the deficiencies in the treatment of the model will remedy this disagreement.

ACKNOWLEDGMENTS

We wish to thank D. C. Tsui for communicating his data to us before publication and helpful discussion during the course of this work. We should like to thank J. M. Rowell for stimulating our interest in this work.

[1]J. R. Schrieffer, in *Semiconductor Surface Physics*, edited by R. H. Kingston (Pennsylvania U. P., Philadelphia, Pa., 1957), p. 55.

[2]P. Handler and S. Eisenhouer, Surface Sci. 2, 64 (1964).

[3]N. St. J. Murphy, Surface Sci. 2, 86 (1964).

[4]S. Kawaji and I. Kawaguchi, J. Phys. Soc. Japan Suppl. 21, 331 (1966).

[5]F. F. Fang and W. E. Howard, Phys. Rev. Letters 16, 797 (1966).

[6]D. C. Tsui, Phys. Rev. Letters 24, 303 (1970).

[7]F. Stern and W. E. Howard, Phys. Rev. 163, 816 (1967).

[8]C. B. Duke, Phys. Rev. 159, 632 (1967).

[9]D. C. Tsui, Bull. Am. Phys. Soc. 16, 143 (1971).

[10]J. J. Quinn and S. Rodriguez, Phys. Rev. 128, 2487 (1962); V. Ya. Demikhovskii and A. P. Protogenov, Fiz. Tverd. Tela 11, 1173 (1969) [Sov. Phys. Solid State 11, 954 (1969)].

[11]D. M. Newns, Phys. Rev. B 1, 3304 (1970).

[12]J. A. Appelbaum and G. A. Baraff, following paper, Phys. Rev. B 4, 1246 (1971).

[13]F. Stern, J. Comp. Phys. 6, 56 (1970).

[14]The use of the WKBJ approximation, using an exponential potential, leads to eigenvalues that agree with that obtained from Schrödinger's equation to better than 1%. Furthermore, the charge density at the origin is at most only 0.2% of its maximum value.